Contents lists available at SciVerse ScienceDirect

Comptes Rendus Geoscience

www.sciencedirect.com

Hydrology, environment

Tectonic control of continental weathering, atmospheric CO_2, and climate over Phanerozoic times

Contrôle tectonique de l'altération continentale, du CO_2 atmosphérique et du climat durant les temps phanérozoïques

Yves Goddéris [a,*], Yannick Donnadieu [b], Vincent Lefebvre [b], Guillaume Le Hir [c], Elise Nardin [a]

[a] CNRS, géosciences environnement Toulouse GET, 14, avenue Édouard-Belin, 31400 Toulouse, France
[b] CNRS, LSCE, 91191 Gif-sur-Yvette cedex, France
[c] IPGP, 1, rue Jussieu, 75238 Paris cedex 05, France

A B S T R A C T

We explore the role of continental drift on the Phanerozoic evolution of the carbon cycle and climate with the GEOCLIM numerical model. GEOCLIM couples a 3D-climate model, a global dynamic vegetation model and a mathematical description of the chemical weathering of the continental surfaces. Twenty-one timeslices covering the whole Phanerozoic are simulated, allowing the calculation of the climate and steady-state atmospheric CO_2 for each of these timeslices. We show that continental drift is a first order control parameter of the geological carbon cycle and climate. The salient features are the following: (1) the Paleozoic environment is characterized by a long term CO_2 decrease; (2) the Late Permian-Late Triassic period displays very high CO_2 levels; (3) atmospheric CO_2 is decreasing since the Middle Cretaceous. All these features are driven by the drift of the continents and the subsequent modulation of the water cycle and weathering rates. Furthermore, continental drift imprints the long term evolution of the tropical seawater surface temperatures with periodical oscillations characterized by a frequency of about 120 Myr, in agreement with available data. Finally, we emphasize a discrepancy existing between the climate reconstructions from the most recent apatite $\delta^{18}O$ data and the CO_2 inferred from proxies. Reconstructed CO_2 levels from proxies are often unrealistically low for the distant geological past.

© 2012 Académie des sciences. Published by Elsevier Masson SAS. All rights reserved.

R É S U M É

Nous explorons le rôle de la dérive des continents sur l'évolution phanérozoïque du cycle du carbone et du climat avec le modèle numérique GEOCLIM. GEOCLIM est un modèle couplant un modèle tridimensionnel du climat, un modèle de la dynamique globale de la végétation et une description mathématique de l'altération chimique des continents. Vingt et une tranches d'âge sont simulées, couvrant l'ensemble du Phanérozoïque, ce qui permet le calcul des conditions climatiques et du niveau de CO_2 d'équilibre pour chacune de ces tranches d'âge. Nous montrons que la dérive des continents est un paramètre de contrôle de premier ordre du cycle du carbone et du climat géologique. Les résultats marquants sont que : (1) l'environnement paléozoïque est caractérisé par une décroissance à long

---

* Corresponding author.
  E-mail address: yves.godderis@get.obs-mip.fr (Y. Goddéris).

terme du niveau de CO$_2$; (2) le niveau de CO$_2$ est très élevé pour la période s'étendant du Permien supérieur au Trias supérieur ; et (3) le niveau de CO$_2$ diminue depuis le milieu du Crétacé. Toutes ces tendances sont pilotées par la dérive des continents et la modulation du cycle de l'eau et des taux d'altération chimique qui en découle. De plus, la dérive des continents imprime à l'évolution à long terme de la température de surface des océans tropicaux une périodicité d'environ 120 Ma, en accord avec les données disponibles. Finalement, nous mettons en lumière un désaccord existant entre les reconstructions climatiques basées sur les plus récentes données δ^{18}O sur apatites et les niveaux de CO$_2$, reconstruits en utilisant les indicateurs disponibles. Les niveaux de CO$_2$ reconstruits à partir des données sont souvent trop bas pour le passé géologique.

1. Introduction

In 1988, Jan Veizer proposed that the time evolution of the surficial envelopes of the Earth was driven by a hierarchy of processes (Veizer, 1988). At the geological timescale (10^6 to 10^9 years), the dominant process controlling the long term changes in the oceanic and atmospheric chemistry, and hence climate, was proposed to be tectonics. In Veizer's view, biological processes are piggybacking on tectonics, and are not driving the long term evolution of the Earth surface. They only adapt to the tectonic forcing. The cross correlation observed between the various isotopic signals measured in Phanerozoic sedimentary carbonates (^{87}Sr/^{86}Sr, δ^{13}C, δ^{18}O) supports this hypothesis (Veizer et al., 1999).

This theory assuming the predominant role of tectonics on the chemical evolution of the Earth surface is challenged by ideas supporting a predominant impact of life on Earth, at least during time periods marked by critical steps in the evolution of life. A well-known example is the accumulation of oxygen in the atmosphere in response to the appearance of the oxygenic photosynthesis. Apparently, subsequent to the oxygenation of the surficial envelopes, atmospheric methane levels decreased drastically, leading to the first severe glaciation at the Earth surface in the Early Proterozoic (Catling and Claire, 2005; Kasting and Ono, 2006; Kopp et al., 2005; Kump, 2008). The invasion of the continental surfaces by land plants during the Devonian is also supposed to have strongly modified the weathering regimes at the Earth surface, and hence the atmospheric CO$_2$ level and the global climate (Berner, 2004). Strikingly, the evolution of life has been proposed also to trigger the onset of cold climatic conditions, here the Permo-Carboniferous glacial event. Terrestrialization may have even impacted the subduction rates, as suggested by non equilibrium thermodynamic considerations (Dyke et al., 2011). In addition, the development of the mycorrhizosphere around plant roots is also thought to have boosted the weathering rates (Taylor et al., 2012). A last example often cited is the evolution of the calcareous nanoplankton which has strongly modified either the chemical gradient in the oceans and possibly the global climate with the emission of dimethyl sulfide into the atmosphere (Westbroeck, 1992).

Is life a climate driver on geological scales, or is tectonics the only forcing function? It is rather difficult to discriminate between the two scenarios. Indeed, for two of the above examples, tectonics may be invoked as the ultimate cause of change, even if life evolution is involved. In the case of the Precambrian oxygen rise, production of oxygen is not sufficient for it to accumulate in the surficial envelopes. It is a matter of relative budget: either the source of O$_2$ must have increased around 2.3 Gyr, or the sink must have declined (Catling and Claire, 2005; Veizer, 1988). For instance, it may be argued that the presence of large continents is required for the nutrients to be supplied by weathering for the biosphere, so that it can support a large oxygen production (Goddéris and Veizer, 2000). Large continents are also required to provide large continental shelves that will be colonized by oxygen producers. So the oxygenation may depend on accretion of new continents around the Archean/Proterozoic boundary that led to transition from the early "mantle-buffered" to the "river-buffered" oceans (Veizer and Mackenzie, 2004), that is, from the scenario where, due to declining geothermal head flux, the early highly reducing fluxes from the ubiquitous submarine hydrothermal circulation cells and volcanism were superposed by more oxidized subaerial volcanism (Kump and Barley, 2007).

Similarly, the rise in nanoplankton producers at the end of the Triassic may have been related in part to changes in carbon cycle and climate linked to the northward drift of Pangea (Goddéris et al., 2008). This latter drift is thought to have enhanced continental rock weathering and associated CO$_2$ consumption, promoting carbonate production in seawater under less acidic conditions. At the same time, coral reefs might have been boosted by this CO$_2$ decrease (Kiessling, 2010). Biological and tectonic forces are also tightly intertwined when considering the role of mountain uplift on the carbon cycle and climate evolution. The proposition that mountain uplift, due to increased erosion, drives CO$_2$ consumption (Raymo and Ruddiman, 1992) and initiates glaciation may be incomplete from the carbon budget perspective because Goddéris and François (1995) and Kump and Arthur (1997) demonstrated that mountain ranges do not increase the overall CO$_2$ consumption by weathering. Instead they may contribute to CO$_2$ drawdown via enhanced regional weatherability that measures susceptibility of a given continental surface to prescribed climatic conditions. Moreover, in the peculiar case of the Himalayan uplift, the high sedimentation rates induced by intense erosion in fact leads to an efficient burial of organic carbon that is mostly of terrestrial origin (France-Lanord and Derry, 1997; Galy et al., 2007). This is another illustration of the tight coupling that may exists between tectonic and biological processes.

2. Aims and method

In this contribution, we aim at isolating the tectonic control on the geological evolution of the carbon cycle and climate. The two main "geological" forcings are tested: the continental drift and the fluctuations in the solid Earth degassing. Although mountain ranges are considered in this study as climatic barriers, we do not account explicitly for their possible geochemical effects such as increased erosion that is potentially promoting organic carbon burial and local weatherability. Nevertheless, physical erosion is accounted for in a simple way (see below).

We use the climate-carbon model GEOCLIM to reconstruct the temporal evolution of the Phanerozoic CO_2 and climate in response to continental drift and to variability in the degassing rate of the solid Earth (Donnadieu et al., 2006, 2009). GEOCLIM couples a 3D climate model (the FOAM GCM; Jacob, 1997) to a model of the global biogeochemical cycles (COMBINE; Goddéris and Joachimski, 2004). For 21 continental configurations spanning the entire Phanerozoic, we calculate the atmospheric CO_2 assuming that the paleothermostat equation is verified (Walker et al., 1981):

$$F_{silw} = F_{vol} \qquad (1)$$

where F_{silw} is the total CO_2 consumption by weathering of continental silicate rocks and F_{vol} the total CO_2 supply from the solid Earth (metamorphism, arc volcanism, mid-oceanic ridge emissions...). Following Berner (2004), F_{vol} is estimated by using a combination of the Gaffin (1987) and Engebretson et al. (1992) reconstructions (Fig. 1).

Nevertheless, it must be kept in mind that this is a parameter still poorly known (Donnadieu et al., 2006).

The specificity of GEOCLIM, compared to other geological climate-carbon models, lies in the method used to calculate F_{silw} (Fig. 2). Different from previous adimensional models (such as GEOCARB, Berner, 2004), GEOCLIM resolves the continental runoff and mean annual air temperature above the continents with a spatial resolution of 7.5° long. × 4.5° lat. (Donnadieu et al., 2006). GEOCLIM is also the only numerical model of its type to allow a process-based calculation of the water cycle. Continental runoff, a key parameter of the weathering reactions, is explicitly calculated by the 3D climate model as the difference between rainfall and evapo-transpiration above each continental grid cell. This allows GEOCLIM to capture accurately the impact of the continental configuration on the runoff pattern. In other models, global runoff is estimated through simple phenomenological laws calibrated on the present continental configuration. The impact of continental drift on runoff is accounted for by offline GCM simulations performed at 1 PAL CO_2, inducing inconsistencies between the calculated state of the carbon cycle and of the climate at each timestep (GEOCARB model; Berner, 2004).

GEOCLIM also includes a dynamic calculation of the distribution of the continental vegetation, via full coupling of the FOAM 3D climate model with the Lund-Postdam-Jena global dynamic vegetation model (Donnadieu et al., 2009). Prior to Devonian, continents are assumed to have been rocky deserts. We are aware that this may be an oversimplification given that early land plants evolved in the Late Ordovician. However, the physical parameters and
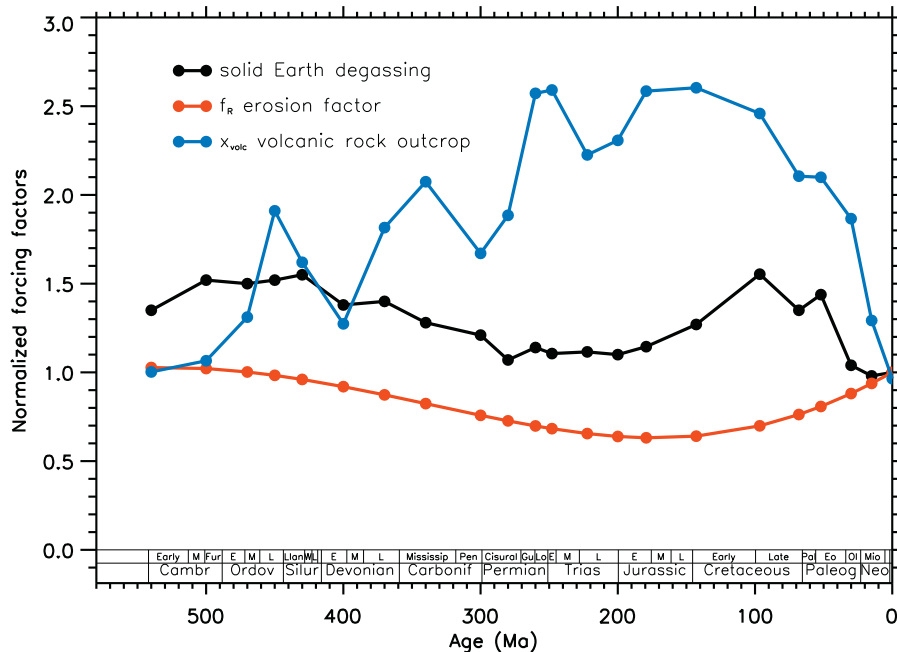

Fig. 1. Three forcing function of the reference simulation. Additional input includes continental configuration and increasing solar constant with time. All functions are normalized to their present day value and taken directly from Berner (2004).

Fig. 1. Les trois fonctions de forçage de la simulation de référence, outre la configuration continentale et la croissance de la constante solaire au cours du temps. Toutes les fonctions sont normalisées à leur valeur actuelle et sont tirées de Berner (2004).
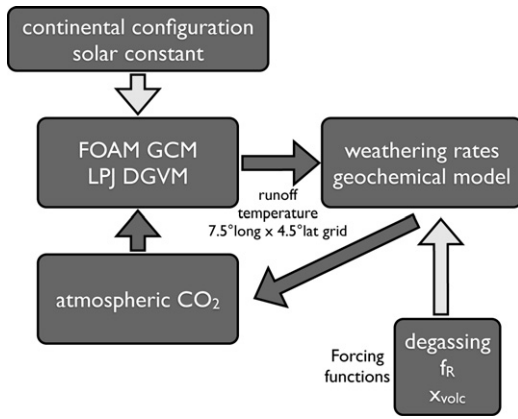
Fig. 2. Description of the GEOCLIM model. For each continental configuration, the climate output of the coupled FOAM climate model and of LPJ dynamic global vegetation model are used to calculate the continental weathering rates, and hence the atmospheric CO_2 level for which consumption by weathering precisely balances the solid Earth outgassing. The three additional forcing function (variable degassing, f_R and x_{volc}) are only used in the reference simulation.

Fig. 2. Description du modèle GEOCLIM. Pour chaque configuration continentale, les sorties climatiques du modèle de climat FOAM couplé au modèle dynamique de végétation globale LPJ sont utilisées pour calculer les taux d'altération continentale, et donc la pression de CO_2 atmosphérique pour laquelle la consommation de CO_2 par altération compense le taux de dégazage volcanique. Les trois fonctions de forçage supplémentaires (dégazage variable, f_R et x_{volc}) ne sont utilisées que pour la simulation de référence.

the spatial extent of this early vegetation are too poorly known to allow a realistic representation in a global numerical model. For Devonian and post-Devonian time-slices, the LPJ model is used with present day plant functional types.

By incorporating a dynamic vegetation in our modeling, we implicitly include an impact of life on the temporal evolution of the global climate. However, we only model the biophysical impact of the vegetation on climate, i.e. changes in albedo and in the roughness of the continental surfaces. The role played by vegetation on the global water cycle is accounted for through modifications of the evaporation capability as a function of the vegetation type. As developed in Donnadieu et al. (2009) and Le Hir et al. (2011), when climate changes in response to continental drift, the distribution of the continental vegetation changes, feedbacking on the climate and water cycle, and hence on the weathering processes. However, in order to limit the biological impact on the long term carbon cycle evolution, we do not account for a direct impact of the biosphere on the weathering rates through time at this stage (enhancement of weathering by root respiration, mechanical effect of roots, release of organic acids).

The F_{silw} term is calculated for each continental grid cell through a parametric relationship linking mean annual runoff and air temperature to CO_2 consumption by weathering (Dessert et al., 2003; Donnadieu et al., 2006; Oliva et al., 2003). Those phenomenological rate laws were calibrated over one hundred small monolithological watersheds, through the measurements of their present day CO_2 consumption by weathering and its correlation

with local runoff and mean annual air temperature. The compiled watersheds span a large variety of climate and vegetation cover. By using these laws even for pre-Devonian times, we implicitly neglect any direct impact of the land plant evolution and root systems on the weathering rates, which makes sense since we aim at isolating as far as possible the tectonic forcing (continental drift) of the climatic evolution of the Earth.

Several modulating factors of weathering rates have been introduced in GEOCLIM if compared to previously published versions. We account for the change in the relative outcrop of young basaltic rocks versus old igneous rocks. Mathematically speaking, the $^{87}Sr/^{86}Sr$ isotopic ratio of sedimentary carbonates is used to estimate x_{volc}, i.e. the ratio of young basaltic rock outcrops versus total continental area (see Berner, 2004 for details; Fig. 1). We also account for a fluctuating role of physical erosion (f_R factor, also taken from the GEOCARB model of Berner, 2004) (Fig. 1). Eq. (1) can thus be rewritten as follows:

$$F_{vol} = \sum_{j=1}^{ncont} \left[k_{shield} \cdot runoff_j \cdot \exp\left(\frac{E_a^{shield}}{R} \left(\frac{1}{T_j} - \frac{1}{T_0} \right) \right) \right]$$
$$\cdot (1 - x_{volc}) \cdot f_R +$$
$$\sum_{j=1}^{ncont} \left[k_{basalt} \cdot runoff_j \cdot \exp\left(\frac{E_a^{basalt}}{R} \left(\frac{1}{T_j} - \frac{1}{T_0} \right) \right) \right] \cdot x_{volc} \cdot f_R$$
(2)

where *ncont* is the number of continental grid cells (around 700, depending on the timeslice), $runoff_j$ and T_j are, respectively, the mean annual runoff and temperature for the grid element *j*. They both depend on the continental configuration and on the solar constant (which are forcing functions), and on the atmospheric CO_2 (the unknown). They are calculated by the 3D climate model. R is the perfect gas constant and T_0 a reference temperature. E_a^{shield} and E_a^{basalt} are the apparent activation energies for shield and basaltic rocks respectively (48 200 and 42 300 J/mol; Dessert et al., 2003; Oliva et al., 2003). k_{shield} and k_{basalt} are calibration constants, set so that basaltic rocks weathering consumes 30% of the total CO_2 consumption by silicate rocks at present (Dessert et al., 2003). Eq. (2) is solved for CO_2 for each of the 21 Phanerozoic timeslices.

3. Results and discussion

3.1. Atmospheric CO_2 levels

Two simulations have been performed. First, the reference simulation assumes a variable solid Earth degassing rate, a variable erosion f_R and a variable young volcanic rocks ratio x_{volc}. Second, the TEC simulation has been run with all these three parameters set at their present day value, allowing us to clearly depict the only effect of continental configuration on atmospheric CO_2.

Regarding the calculated atmospheric CO_2 content, the salient features of both simulations can be summarized as follows (Fig. 3):

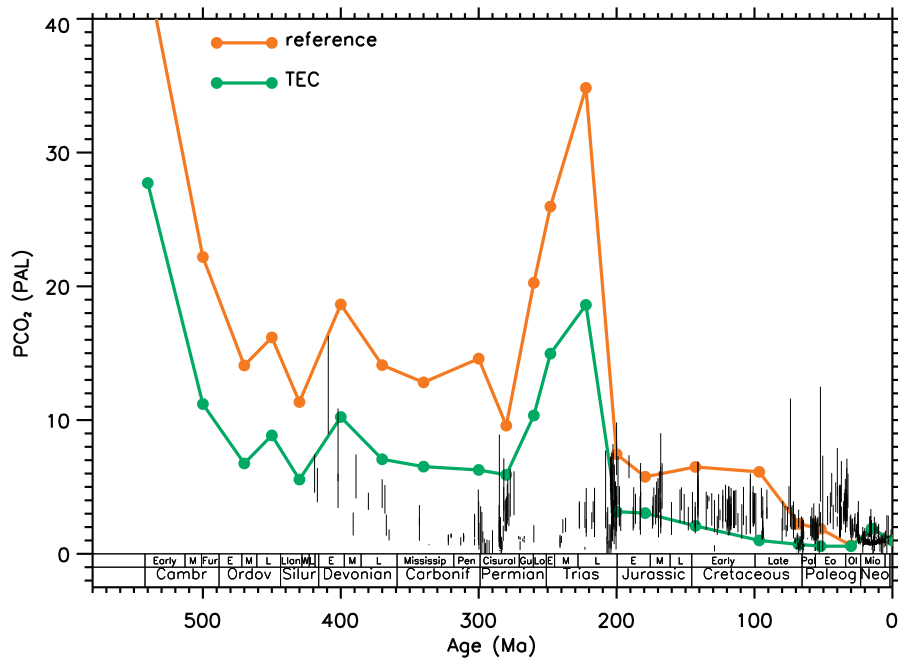• the Early Paleozoic period is characterized by a major atmospheric CO_2 decrease;

Fig. 3. Calculated evolution of the atmospheric CO_2 pressure over time, using the GEOCLIM model for the reference and the TEC (where the only forcings are the continental configuration and the solar constant) simulations (1 PAL = 280 ppmv). Also shown (vertical black lines) is the latest update of the CO_2 proxy database (Breecker et al., 2010; Royer et al., 2007).

Fig. 3. Évolution calculée par le modèle GEOCLIM de la pression de CO_2 atmosphérique, pour les simulations de référence et TEC (pour laquelles les deux seuls forçages sont la configuration continentale et la constante solaire) (1 PAL = 280 ppmv). La dernière version de la base de données du niveau de CO_2 est également figurée (barres verticales noires) (Breecker et al., 2010 ; Royer et al., 2007).

- the Triassic and the Cambrian are marked by very high CO_2 levels;
- since the Middle Cretaceous (around 100 Ma in the reference run, slightly earlier in the TEC run which displays overall lower CO_2 levels), the calculated CO_2 level is rapidly declining from 6 PAL (reference run) down to the present day value.

In detail, the high Paleozoic values are mainly forced by the low solar constant. Atmospheric CO_2 is forced to rise to compensate for the low insolation, so that silicate weathering is sustained and the paleothermostat equation is verified (Eq. (1) and (2)). However, a major drop in CO_2 levels is calculated from the Mid-Ordovician to the Llandovery. The cause of this drop is of tectonic origin. In detail, this is the northward drift of the three main continental blocks (Laurentia, Siberia and Baltica) that maximizes the CO_2 consumption by silicate weathering, forcing atmospheric CO_2 to decrease and climate to get colder (Nardin et al., 2011).

The second period when continental configuration plays a dominant control on the global carbon cycle is the Triassic. Very high CO_2 levels are calculated from the Lopingian period up to the Carnian stage of the Triassic, from about 5500 up to 9800 ppmv. These high CO_2 levels are directly related to the shaping of the Pangea supercontinent at the same time. Because of increasing continentality, runoff is maintained at low levels, and the climate system warms so that temperature and runoff are eventually high enough for silicate weathering to

compensate for the solid Earth degassing (Donnadieu et al., 2006; Gibbs et al., 1999; Goddéris et al., 2008). These high levels are sustained as long as the supercontinental configuration inhibits runoff. In the latest stage of the Triassic (Rhetian), the northward drift of Pangea increases the continental surface located in the intertropical convergence zone, thus promoting silicate weathering and forcing CO_2 to decrease (Goddéris et al., 2008). After the Latest Triassic, persisting low CO_2 levels are maintained by the fragmentation of the Pangea, promoting runoff, and hence silicate weathering.

The latest marked event is the decrease in atmospheric CO_2 over the last 100 million years (150 million years in the TEC run). Although it may appear moderate compared to older CO_2 excursions, its climatic impact is important given that climate sensitivity increases at low CO_2 levels because of the logarithmic dependence of the climate on the CO_2 level. This continental weatherability increase and subsequent CO_2 decrease are the consequences of the ongoing breakup of the Pangea. Following the opening of the South Atlantic after the Berriasian, the northern part of Africa and South America stays in the convergence zone during this period, allowing an intense CO_2 consumption by weathering (Fig. 4).

3.2. Temperature trends

A striking feature of the reference simulation is the prediction of the lowest global temperature in the Late Cenozoic (Fig. 5). All other periods of the Phanerozoic are
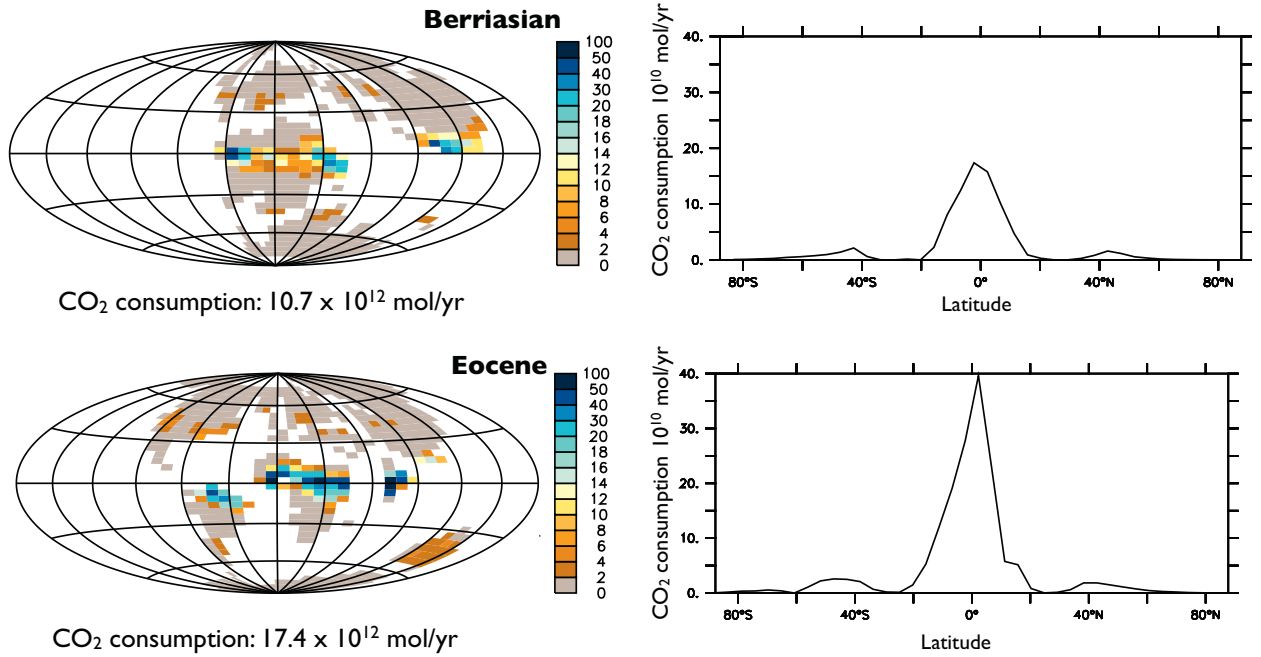
Fig. 4. Calculated CO$_2$ consumption by silicate weathering for the Berrisian stage of the Cretaceous to the Eocene. Calculations were performed under 1 PAL (280 ppmv) of atmospheric CO$_2$. Shown is the spatial and latitudinal distribution of the flux, on 10^{10} mol of CO$_2$/yr. The number is the total CO$_2$ consumption in 10^{12} mol/yr, illustrating the weatherability increase from the Cretaceous towards the Cenozoic.

Fig. 4. Consommation de CO$_2$ par l'altération des silicates pour l'étage Berriasien du Crétacé et pour l'Éocène. Les calculs ont été effectués pour une pression de 280 ppmv de CO$_2$ atmosphérique (1 PAL). La distribution spatiale et la répartition en latitude du flux sont montrées en 10^{10} mol CO$_2$/an. Le nombre isolé donne la consommation totale de CO$_2$ en 10^{12} mol/an, illustrant l'augmentation de l'altérabilité du Crétacé au Cénozoïque.
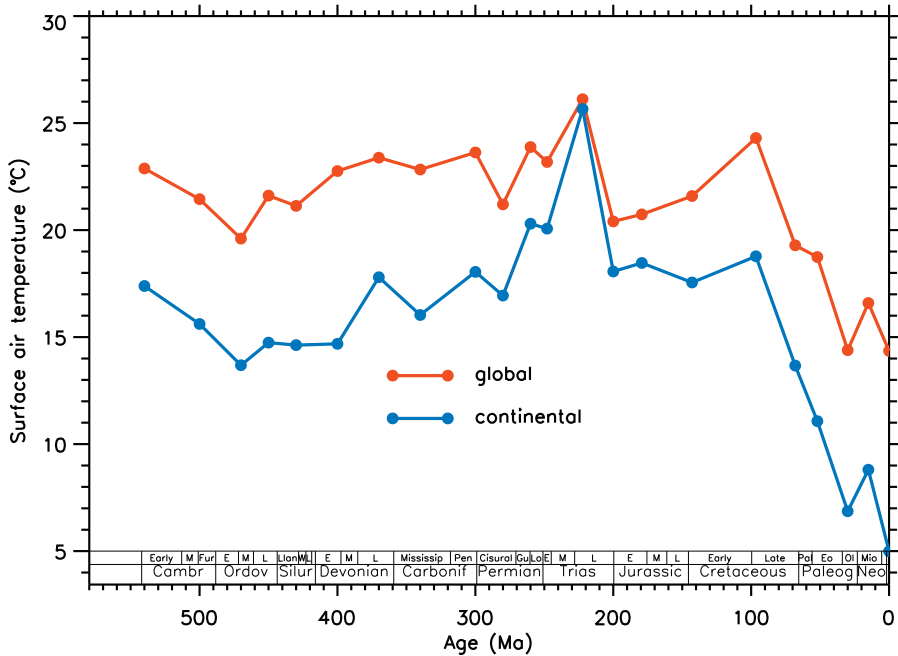

Fig. 5. Calculated time evolution of the global mean air temperature and continental mean air temperature, for the reference simulation.

Fig. 5. Évolution temporelle calculée de la température moyenne de l'air globale et continentale dans la simulation de référence.
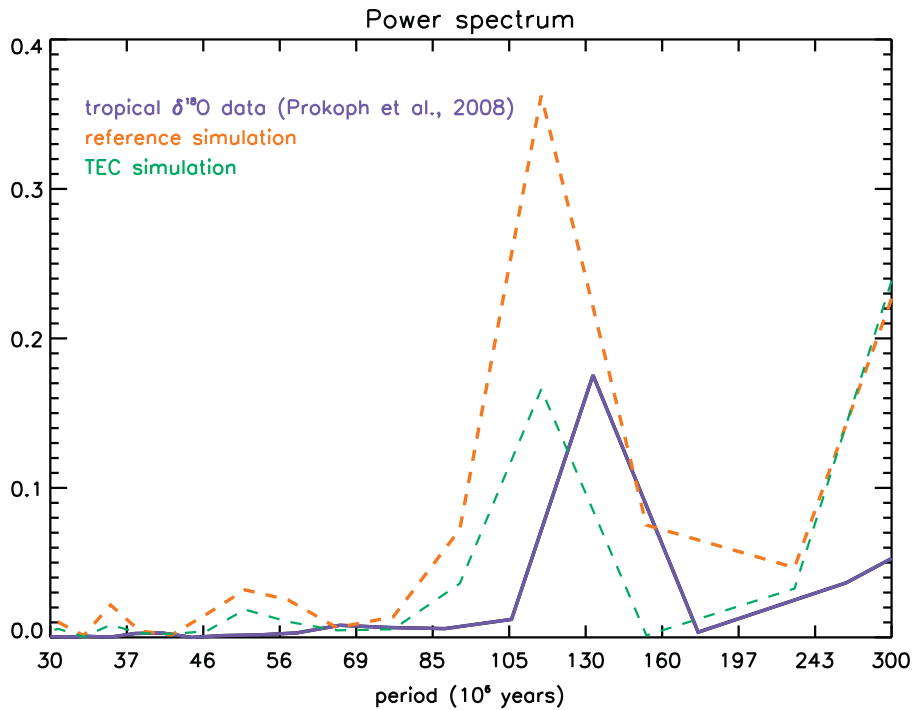
Fig. 6. Power spectrum of the Fourier analysis of the averaged tropical sea surface temperature (30°S–30°N) calculated in the reference and TEC simulations. Data are from Prokoph et al. (2008) and based on carbonate δ¹⁸O.

Fig. 6. Spectre de puissance résultant de l'analyse de Fourier de la température moyenne des eaux de surface tropicales (30°S–30°N), calculée dans les simulations de référence et TEC. Les données de δ¹⁸O acquises sur carbonates sédimentaires proviennent de Prokoph et al. (2008).
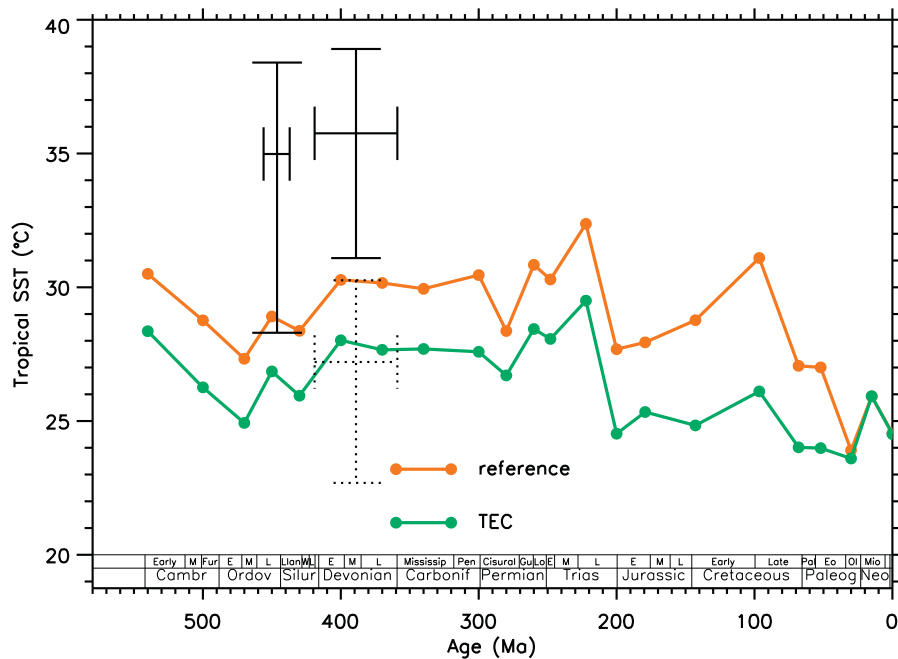

Fig. 7. Averaged tropical sea surface temperature calculated in the reference and TEC simulations. The crosses stand for data (conodont apatite δ¹⁸O data for the Devonian, Joachimski et al., 2009 with the Pucéat et al. (2010) new paleothermometer; Δ⁴⁷ data for the Ordovician from Finnegan et al., 2011). The dotted cross represents temperature for the Devonian when the Kolodny et al. (1983) paleothermometer is used.

Fig. 7. Température moyenne des eaux tropicales de surface, calculée dans les simulations de référence et TEC. Les croix représentent les températures reconstruites à partir des données δ¹⁸O sur conodontes pour le Dévonien (Joachimski et al., 2009) (avec le paléothermomètre de Pucéat et al. (2010)), et des données Δ⁴⁷ pour l'Ordovicien (Finnegan et al., 2011). La croix en pointillés représente la température moyenne pour le Dévonien, quand le paléothermomètre de Kolodny et al. (1983) est utilisé.

predicted to be warmer by at least 5 °C. The same conclusion holds for the continental temperature with the Oligocene, Miocene and present day temperatures about 8 °C below the Paleozoic-Mesozoic mean value. The warmest continents are predicted in the Middle Triassic, with a mean annual temperature in excess of 25 °C.

Comparing these temperature outputs to available data (from $\delta^{18}O$ measured on sedimentary apatite or carbonate) might not be fully relevant. Indeed, our model only calculates the multi-million year steady-state CO_2, corresponding to the climate required for silicate weathering to balance the volcanic outgassing. Many other possible forcing functions are missing, such as the organic carbon burial and its impact on the global carbon cycle.

However, trends can be identified. We performed a frequency analysis of the temperature calculated for the tropical surface ocean (30°N–30°S) over the whole Phanerozoic in the standard simulation. The spectrum shows the dominance of the 115 Myr period, close to the 132 Myr period calculated from the Phanerozoic $\delta^{18}O$ database for the tropical seawater (Prokoph et al., 2008)

and to the 135 Myr calculated by Veizer et al. (2000) from an older version of the $\delta^{18}O$ database (Fig. 6). This periodicity, observed also in the compilation of Phanerozoic glacial deposits (Frakes et al., 1992; Veizer et al., 2000) was never explained before. Our results suggest that it may be linked to the continental drift and its control on the weathering fluxes. Indeed, if we assume a constant degassing rate, a constant x_{volc} and f_R (both fixed at their present day value), the only remaining forcings are the linear rise in the solar constant and the continental drift (TEC simulation). The sea surface tropical temperature calculated by GEOCLIM still displays a strong periodicity signal at 115 Ma (Fig. 6). Consequently, the continental drift over the Phanerozoic, by successively promoting or inhibiting continental weathering, strongly contributes to the observed periodicity of the tropical temperature signal.

4. Temperature and CO_2 changes over time

Is it possible to estimate the absolute CO_2 level in the past? Many studies have dealt with this question from a
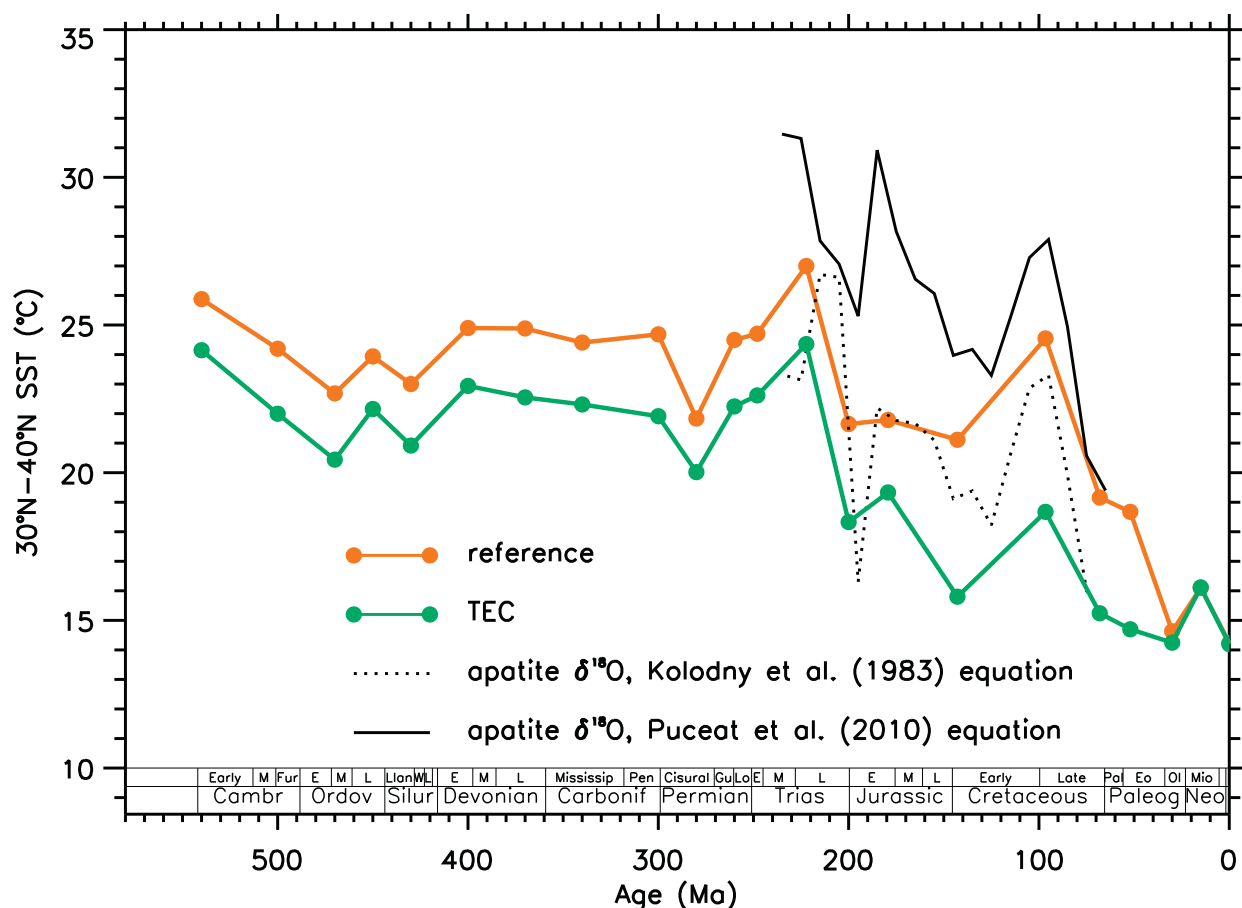

Fig. 8. Averaged surface seawater temperatures between 30°N–40°N latitude for the reference and TEC simulations. The black lines stand for the temperatures reconstructed from apatite $\delta^{18}O$ data, compilation by E. Pucéat (personal communication), with two different paleothermometers.

Fig. 8. Températures moyennes d'eaux de surface entre les latitudes 30°N–40°N, calculées dans les simulations de référence et TEC. Les lignes noires montrent la température reconstruite à partir des données $\delta^{18}O$ sur apatite sédimentaire, avec deux paléothermomètres différents (compilation par E. Pucéat, communication personnelle).

proxy point of view. Absolute CO_2 levels have been reconstructed over the last 450 million years from stomatal index of fossil leaves, from $\delta^{13}C$ of pedogenic carbonates, from the biospheric carbon isotopic fractionation in the ocean among other methods (Royer et al., 2001). While those proxies can provide very different results (Goddéris et al., 2008), publications of the last years tend to lower the estimates of CO_2. For instance, despite the existence of studies showing high levels of CO_2 in the Middle Miocene (Kürschner et al., 2008), there is a real fascination for studies suggesting very low levels during this warm interval (below the pre-industrial value, Pagani et al., 2005). Recently, Breecker et al. (2010) have drastically reduce the Paleozoic and Mesozoic CO_2 values through a recalibration of the pedogenic carbonate method. We are now left with level as low as 1000 ppmv in the Devonian, or below 1000 ppmv in the Early Triassic (Fig. 3).

Conversely, seawater temperatures calculated from proxies for the deep time tends to increase in the most recently published dataset. Ten years ago, the $\delta^{18}O$ carbonate data predict very high temperatures in the seawater, particularly for the Paleozoic, because they display a general decreasing trend as we go back into the past (Veizer et al., 1999). However, $\delta^{18}O$ ratio measured on well preserved apatite (mainly conodonts for the Paleozoic, then fish teeth for more recent periods) suggested lower temperatures than coeval carbonate samples, casting doubt on the reliability of the carbonate data. However, a recent recalibration of the apatite paleothermometer by Pucéat et al. (2010) warms up apatite-based temperatures by at least 4 °C, so that they display now high temperatures, close

to the temperatures inferred from carbonate data. For instance, tropical sea surface temperatures reconstructed from conodont apatite now reaches 37 to 38 °C in the Devonian when the new paleothermometer is used (Fig. 7), while it was never exceeding 32 °C (Joachimski et al., 2009) with the former paleothermometer (Kolodny et al., 1983). Such high temperatures cannot be reached with only 1000 ppmv of CO_2, given that the solar constant is reduced by 3%. For instance, GEOCLIM calculates a mean tropical SST of only 30 °C with more than 4200 ppmv of CO_2 (15 PAL). Regarding the Triassic, our model correctly reproduced the high temperatures inferred from apatite $\delta^{18}O$ (27 to 28 °C) for the latitude zone extending from 30°N to 40°N, but the CO_2 level required to do so is close to 10 000 ppmv, far above the CO_2 estimated from proxies (around 1000 ppmv) (Fig. 8). The same conclusion applies to the Jurassic and Middle Cretaceous. The CO_2 levels required to reproduce the best available temperature dataset are above the proxy-based CO_2. So there is something wrong: the data-based temperatures or the proxy-based CO_2 levels or the model CO_2 sensitivity, or even all of them.

The problem may be rooted in the CO_2 proxies. Indeed, as emphasized by Huber and Caballero (2011), the calibration of the leaf stomatal index method at high CO_2 is weakly constrained and recent evidence that leaves adapt not only the size of the stomata but also their density at high CO_2 values (Franks and Beerling, 2009) raises questions about the validity of the proxy at high CO_2. Indeed, as recently affirmed by Smith et al. (2010), the stomatal methods should probably be considered semi-quantitative under high CO_2 conditions and may represent CO_2 minima. We also have to acknowledge that several
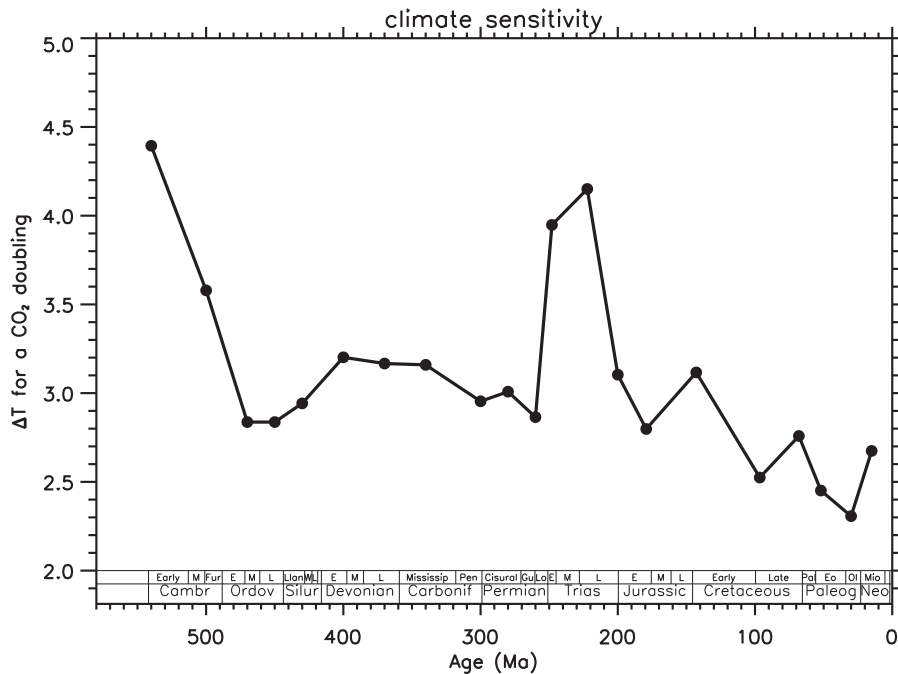

Fig. 9. Mean global air temperature sensitivity of the FOAM climate model to a CO_2 doubling as a function of the geological age.

Fig. 9. Sensibilité de la température moyenne globale de l'air calculée par le modèle climatique FOAM à un doublement de CO_2 atmosphérique, en fonction de l'âge géologique.

unconstrained parameters are deeply rooted in the pedogenic carbonate method; the most critical is the fraction of below ground CO_2 respired by land plants (Royer et al., 2001) for the distant geological past.

Another cause of the apparent temperature-CO_2 paradox might be the model climate sensitivity. Here, the response of the mean global air temperature to a CO_2 doubling is a function of the continental configuration (Fig. 9). It reaches a maximum of 4 °C during the Triassic (Pangea configuration) and when most of the continents are located around the South pole (beginning of the Phanerozoic). Then it fluctuates between 2.3 and 3 °C for other periods. Two conclusions arise from this. First, since the climate sensitivity is a function of the continental configuration, we think that using the reconstructions of past geological climates to constrain the future climate sensitivity must be undertaken with an extreme caution, particularly for the Mesozoic and Paleozoic climates (Royer et al., 2007). Park and Royer (2011) found a roughly constant sensitivity at 3 to 4 °C, except during ice ages where the sensitivity rises. Here, accounting physically for the impact of the continental configuration, the picture appears rather different: we found that the sensitivity is highest during periods characterized by supercontinental or "polar-location" configurations (where large continents are located at high latitudes), while other periods display a sensitivity at the lower band of the Park and Royer estimates. Second, the climate model used in this study has a sensitivity which is not anomalously low, given what is known of the climate behavior (Meehl et al., 2007), so that the question of the discrepancy between proxy-based temperatures and CO_2 remains unsolved.

5. Conclusions and future research directions

In this contribution, we estimated the atmospheric CO_2 levels for 21 Phanerozoic timeslices, using a coupled 3D climate and carbon-alkalinity model (GEOCLIM). Our aim was to explore the role of the tectonic drift on the time evolution of the CO_2 level at the Phanerozoic timescale. Compilation of several of our previous studies in combination with new simulations, led us to suggest that the Phanerozoic tectonic drift induces a periodic climatic signal, alterning warmer and colder periods with a periodicity of about 115 Myr, in close agreement with the climatic periodicity inferred from glacial deposit inventory (Frakes et al., 1992) and from carbonate $\delta^{18}O$ data (Veizer et al., 2000).

The paleogeographic configuration also forces the atmospheric CO_2 to high levels in the Early Paleozoic and within a time window from the Late Permian to the Late Triassic. This time window is interesting. The tectonic drift may explain by itself why this period was warm, mainly because it was dry, a state inhibiting CO_2 consumption by continental weathering. Although this warm interval is recorded in many climatic indexes, including $\delta^{18}O$ data (Prokoph et al., 2008; Veizer et al., 2000), it is totally absent from the CO_2 proxy-based curve. This particular case illustrates a general discrepancy existing between the proxy-based CO_2 levels and the reconstructed Phanerozoic climates. The proxy-based CO_2 levels are generally too low to explain the observed climatic features.

One last conclusion is that the distant past might not be the key to the future. We show that the climate sensitivity to atmospheric CO_2 depends on the paleogeographic configuration, being maximal (4 °C for a CO_2 doubling) during supercontinental configurations or when continents are mostly located at high latitudes.

In the future, similar studies should be performed with other general circulation models. We must be aware that the vast majority of deep time climatic studies were performed with the GENESIS GCM, while we used another 3D FOAM GCM climate model. Each of these models has its own limitations. For climate studies dealing with the future evolution of the Earth system, the Intergovernmental Panel on Climate Change (IPCC) uses a large variety of models in order to estimate the inherent uncertainties (Meehl et al., 2007) and we believe that such a procedure should be employed also for the study of the coupled evolution of the carbon cycle and climate in the past.

References

Berner, R.A., 2004. The Phanerozoic carbon cycle. Oxford University Press, New York, 150 p.

Breecker, D.O., Sharp, Z.D., McFadden, L.D., 2010. Atmospheric CO_2 concentrations during ancient greenhouse climates were similar to those predicted for A.D. 2100. Proc. Natl. Acad. Sci. 107, 576–580.

Catling, D.C., Claire, M.W., 2005. How Earth's atmosphere evolved to an oxic state: a status report. Earth Planet Sci. Lett. 237, 1–20.

Dessert, C., Dupré, B., Gaillardet, J., François, L.M., Allègre, C.J., 2003. Basalt weathering laws and the impact of basalt weathering on the global carbon cycle. Chem. Geol. 202, 257–273.

Donnadieu, Y., Goddéris, Y., Pierrehumbert, R., Dromart, G., Fluteau, F., Jacob, R., 2006. A GEOCLIM simulation of climatic and biogeochemical consequences of Pangea breakup. Geochem. Geophys. Geosys. 7, 1–21 doi:10.1029/2006GC001278.

Donnadieu, Y., Goddéris, Y., Bouttes, N., 2009. Exploring the climatic impact of the continental vegetation on the Mesozoic atmospheric CO_2 and climate history. Climate Past 5, 85–96.

Dyke, J.G., Gans, F., Kleidon, A., 2011. Towards understanding how surface life can affect interior geological processes: a non-equilibrium thermodynamics approach. Earth Syst. Dynam. 2, 139–160.

Engebretson, D.C., Kelley, K.P., Cashman, H.J., Richards, M.A., 1992. 180 million years of subduction. GSA Today 2, 93–95.

Finnegan, S., Bergmann, K., Eiler, J.M., Jones, D.S., Fike, D.A., Eisenman, I., Hughes, N.C., Tripati, A.K., Fischer, W.W., 2011. The magnitude and duration of Late Ordovician-Early Silurian glaciation. Science 331, 903–906.

France-Lanord, C., Derry, L.A., 1997. Organic carbon burial forcing of the carbon cycle from Himalayan erosion. Nature 390, 65–67.

Franks, P.J., Beerling, D.J., 2009. Maximum leaf conductance driven by CO_2 effects on stomatal size abd density over geologic time. Proc. Natl. Acad. Sci. 106, 10343–10347.

Frakes, L.A., Francis, J.E., Syktus, J.I., 1992. Climate modes of the Phanerozoic. Cambridge University Press, Cambridge.

Gaffin, S., 1987. Ridge volume dependence on seafloor generation rate and inversion using long term sealevel change. Am. J. Sci. 287, 596–611.

Galy, V., France-Lanord, C., Beyssac, O., Faure, P., Kudrass, H., Palhol, F., 2007. Efficient organic carbon burial in the Bengal fan sustained by the Himalayan erosional system. Nature 450, 407–410.

Gibbs, M.T., Bluth, G.J.S., Fawcett, P.J., Kump, L.R., 1999. Global chemical erosion over the last 250 My: variations due to changes in paleogeography, paleoclimate, and paleogeology. Am. J. Sci. 299, 611–651.

Goddéris, Y., François, L.M., 1995. The Cenozoic evolution of the strontium and carbon cycles: relative importance of continental erosion and mantle exchanges. Chem. Geol. 126, 169–190.

Goddéris, Y., Veizer, J., 2000. Tectonic control of chemical and isotopic composition of ancient oceans: the impact of continental growth. Am. J. Sci. 300, 434–461.

Goddéris, Y., Joachimski, M.M., 2004. Global change in the Late Devonian: modelling the Frasnian-Famennian short-term carbon isotope excursions. Palaeogeogr., Palaeoclimatol., Palaeoecol. 202, 309–329.

Goddéris, Y., Donnadieu, Y., de Vargas, C., Pierrehumbert, R.T., Dromart, G., van de Schootbrugge, B., 2008. Causal or casual link between the rise of nannoplankton calcification and a tectonically-driven massive decrease in Late Triassic atmospheric CO_2? Earth Planet Sci. Lett. 267, 247–255.

Huber, M., Caballero, R., 2011. The Early Eocene equable climate problem revisited. Climate Past 7, 603–633.

Jacob, R., 1997. Low frequency variability in a simulated atmosphere ocean system. PhD thesis. Univ. Wisconsin, Madison.

Joachimski, M.M., Breisig, S., Buggish, W., Talent, J.A., Mawson, R., Gereke, M., Morrow, J.R., Day, J., Weddige, K., 2009. Devonian climate and reef evolution: insights from oxygen isotopes in apatite. Earth Planet Sci. Lett. 284, 599–609.

Kasting, J.F., Ono, S., 2006. Palaeoclimates: the first two billion years. Phil. Trans. R. Soc. B 361, 917–929.

Kiessling, W., 2010. Reef expansion during the Triassic: spread of photosymbiosis balancing climatic cooling. Palaeogeogr., Palaeoclimatol., Palaeoecol. 290, 11–19.

Kolodny, Y., Luz, B., Navon, O., 1983. Oxygen isotope variations in phosphate of biogenic apatite. I. Fish bone apatite - rechecking the rules of the game. Earth Planet Sci. Lett. 64, 398–404.

Kopp, R.E., Kirschvink, J.L., Hillburn, I.A., Nash, C.Z., 2005. The Paleoproterozoic snowball Earth: a climate disaster triggered by the evolution of oxygenic photosynthesis. Proc. Natl. Acad. Sci. 102, 11131–11136.

Kump, L.R., 2008. The rise of atmospheric oxygen. Nature 451 doi:10.1038/nature06587.

Kump, L.R., Arthur, M.A., 1997. Global chemical erosion during the Cenozoic: weatherability balances the budget. In: Ruddiman, W.F. (Ed.), Tectonic and climate change. Plenum Press, New York, pp. 399–426.

Kump, L.R., Barley, M.E., 2007. Increased subaerial volcanism and the rise of atmospheric oxygen 2.5 billion years ago. Nature 448, 1033–1036.

Kürschner, W.M., Kvaček, Z., Dilcher, D.L., 2008. The impact of Miocene atmospheric carbon dioxide fluctuations on climate and the evolution of terrestrial ecosystems. Proc. Natl. Acad. Sci. 105, 449–453.

Le Hir, G., Donnadieu, Y., Goddéris, Y., Meyer-Berthaud, B., Ramstein, G., Blakey, R.C., 2011. The climate change caused by the land plant invasion in the Devonian. Earth Planet Sci. Lett. 310, 203–212.

Meehl, G.A., Stocker, T.F., Collins, W.D., Friedlingstein, P., Gaye, A.T., Gregory, J.M., Kitoh, A., Knutti, R., Murphy, J.M., Noda, A., Raper, S.C.B., Watterson, I.G., Weaver, A.J., Zhao, Z.-C., 2007. Global climate projections. Climate change 2007: the physical basis. In: Solomon, S., Qin, D., Manning, M., Chen, Z., Marquis, M., Averyt, K.B., Tignor, M., Miller, H.L. (Eds.), Contribution of working group I to the fourth assessment report of the Intergovernementl Panel on Climate Change. Cambridge University Press, Cambridge, United Kingdom and New York, NY, USA.

Nardin, E., Goddéris, Y., Donnadieu, Y., Le Hir, G., Blakey, R.C., Pucéat, E., Aretz, M., 2011. Modeling the Early Paleozoic long-term climatic trend. GSA Bull. 123, 1181–1192.

Oliva, P., Viers, J., Dupré, B., 2003. Chemical weathering in granitic environments. Chem. Geol. 202, 225–256.

Pagani, M., Zachos, J.C., Freeman, K.H., Tipple, B., Bohaty, S., 2005. Marked decline in atmospheric carbon dioxide concentrations during the Paleogene. Science 309, 600–603.

Park, J., Royer, D.L., 2011. Geologic constraints on the glacial amplification of Phanerozoic climate sensitivity. Am. J. Sci. 311, 1–26.

Prokoph, A., Shields, G.A., Veizer, J., 2008. Compilation and time-series analysis of a marine carbonate $\delta^{18}O$, $\delta^{13}C$, $^{87}Sr/^{86}Sr$ and $\delta^{34}S$ database through Earth history. Earth Sci. Rev. 87, 113–133.

Pucéat, E., Joachimski, M.M., Bouilloux, A., Monna, F., Bonin, A., Motreuil, S., Morinière, P., Hénard, S., Mourin, J., Dera, G., Quesne, D., 2010. Revised phosphates-water fractionation equation reassessing paleotemperatures derived from biogenic apatite. Earth Planet Sci. Lett. 298, 135–142.

Raymo, M.E., Ruddiman, W.F., 1992. Tectonic forcing of the Late Cenozoic climate. Nature 359, 117–122.

Royer, D.L., Berner, R.A., Beerling, D.J., 2001. Phanerozoic atmospheric CO_2 change: evaluating geochemical and paleobiological approaches. Earth Sci. Rev. 54, 349–392.

Royer, D.L., Berner, R.A., Park, J., 2007. Climate sensitivity constrained by CO_2 concentrations over the past 420 million years. Nature 446, 530–532.

Smith, R.Y., Greenwood, D.R., Basinger, J.F., 2010. Estimating paleoatmospheric pCO_2 during the Early Eocene Climatic Optimum from stomatal frequency of Gingko, Okanagan Highlands, British Columbia, Canada. Palaeogeogr., Palaeoclimatol., Palaeoecol. 293, 120–131.

Taylor, L.L., Banwart, S.A., Valdes, P.J., Leake, J.R., Beerling, D.J., 2012. Evaluating the effects of terrestrial ecosystems, climate and carbon dioxide on weathering over geological time: a global-scale process-based approach. Phil. Trans. R. Soc. B 367, 565–582.

Veizer, J., 1988. The Earth and its life: systems perspective. Orig. Life Evol. Biosph. 18, 13–39.

Veizer, J., Goddéris, Y., François, L.M., 2000. Evidence for decoupling of atmospheric CO_2 and global climate during the Phanerozoic eon. Nature 408, 698–701.

Veizer, J., Ala, D., Azmy, K., Bruckschen, P., Buhl, D., Bruhn, F., Carden, G.A.F., Diener, A., Ebneth, S., Goddéris, Y., Jasper, T., Korte, C., Pawellek, F., Podlaha, O.G., Strauss, H., 1999. $^{87}Sr/^{86}Sr$, $\delta^{13}C$ and $\delta^{18}O$ evolution of Phanerozoic seawater. Chem. Geol. 161, 59–88.

Veizer, J., Mackenzie, F.T., 2004. Evolution in sedimentary rocks. In: Holland, H.D., Turekian, K.K. (Eds.), Treatise on Geochemistry, vol. 7. Elsevier, pp. 369–407.

Walker, J.C.G., Hays, P.B., Kasting, J.F., 1981. A negative feedback mechanism for the long-term stabilization of Earth's surface temperature. J. Geophys. Res. 86, 9776–9782.

Westbroeck, P., 1992. Life as a geological force: dynamics of the Earth. WW Norton & Company, New York, 240 p.